

Original Article



Synthesis and Evaluation of a Novel Small-molecule Compound as an Anticancer Inhibitor of CD147*

FU Zhi Guang^{1,2,&}, WANG Yan^{3,&}, WANG Shuang⁴, SHAO Dan⁴, TIAN Li⁵, LI Yun Xia⁶,
JIANG Jian Li^{2,#}, CHEN Zhi Nan^{2,#}, and WEN Ning^{1,#}

1. Department of Stomatology, Chinese PLA General Hospital, Beijing 100850, China; 2. Cell Engineering Research Center & Department of Cell Biology, State Key Laboratory of Cancer Biology, National Key Discipline of Cell Biology, Fourth Military Medical University, Xi'an 710032, Shaanxi, China; 3. Department of Internal Neurology, 309 Hospital of PLA, Beijing 100091, China; 4. Department of Stomatology, Huangdao District Central Hospital, Qingdao, 266000, Shandong, China; 5. Department of Anesthesiology & Perioperative Medicine, Xijing Hospital, Fourth Military Medical University, Xi'an 710032, Shaanxi, China; 6. Outpatient Department, Special Police College of the Chinese Armed Police Force, Beijing 100621, China

Abstract

Objective Cancer is a serious threat to human health. Despite extensive research on cancer treatment, there is a growing demand for new therapies. CD147 is widely involved in tumor development, but it is unclear whether cancer cell malignancy is affected by CD147 expression level. The first compound (AC-73) targeting CD147 could only act on advanced tumors and inhibit metastasis. Therefore, new compounds with better anticancer activity should be explored.

Methods Wst-1 assays were used to confirm the effect of novel compounds on proliferation. Apoptosis tests were used to evaluate their proapoptotic capacity. A nude mouse model was used to demonstrate *in vivo* anticancer activity and safety of the compounds. Western blots were used to suggest a molecule mechanism.

Results There is a positive correlation between CD147 expression and tumor cell proliferation. A new compound, HA-08, was synthesized and proved to be more active than AC-73. HA-08 could inhibit cancer cell viability and promote cancer cell apoptosis both *in vitro* and *in vivo*. HA-08 induces cancer apoptosis, mainly by disrupting the CD147-CD44 interaction and then down-regulating the JAK/STAT3/Bcl-2 signaling pathway.

Conclusion Our results have clarified the tumor specificity of CD147 and its drug target characteristics. The biological profile of HA-08 suggests that this compound could be developed as a potential anticancer agent.

Key words: Antigens; CD147; Antineoplastic agents; Apoptosis

Biomed Environ Sci, 2019; 32(9): 673-686 doi: 10.3967/bes2019.086

ISSN: 0895-3988

www.besjournal.com (full text)

CN: 11-2816/Q

Copyright ©2019 by China CDC

*This work was supported by grants from the National Natural Science Foundation of China [grant number 81703003, Z.G. Fu and grant number 81700968, P. X] and a China Postdoctoral Science Foundation Funded Project [Project No.: 2017M623395 and Project No.: 2018T111143].

&These authors contributed equally to this work.

#Correspondence should be addressed to JIANG Jian Li, E-mail: jiangjl@fmmu.edu.cn, Tel: 86-29-84773243; CHEN Zhi Nan, E-mail: znchen@fmmu.edu.cn, Tel: 86-29-84773863; WEN Ning, E-mail: wenningchn@163.com, Tel: 86-10-66937179

Biographical notes of the first authors: FU Zhi Guang, male, born in 1986, PhD, majoring in targeted cancer therapy; WANG Yan, female, born in 1987, Attending Doctor, majoring in neuroscience.

INTRODUCTION

Cancer remains a major global public health problem. As the second leading cause of death worldwide, after heart disease, cancer poses a great challenge to the field of medicine. For several years, traditional chemotherapy, as well as radiation therapy and surgery, have been the main treatment modalities for cancer patients^[1-3]. The major drawback of current cancer therapies is the inability to deliver specific drugs to the target, causing them to affect both healthy and cancerous cells^[4,5]. Therefore, it is critical to develop new strategies for cancer therapy.

Targeted cancer therapies (TCTs) have emerged as some of the most promising treatments for cancer patients in recent years^[6]. Different types of TCT drugs such as monoclonal antibodies (mAbs) and small-molecule inhibitors (SMIs) have been shown to control the progression of various cancers^[7,8]. However, the potential immunogenicity of most mAbs, which results in the development of human anti-mouse antibodies (HAMAs), needs to be prevented. In addition, most targets of SMIs are protein kinases, which are not always tumor-specific^[9]. These factors may lead to unexpected side effects. Therefore, novel TCT drugs are likely to be developed, and new tumor-specific molecules need to be identified as potential targets for tumor therapy.

CD147 is a multifunctional transmembrane protein with two extracellular Ig-like domains and a cytoplasmic tail consisting of 40 amino acids^[10]. CD147 has been reported to be overexpressed in nearly 20 tumor types^[11]. In addition, CD147 is highly involved in biological tumor-related events such as tumorigenesis, invasion and impaired metabolism, among others^[12-16]. These findings suggest that CD147 can be characterized as a largely tumor-specific molecule. Based on these findings, we previously identified the first small-molecule compound that targets CD147, called AC-73, which prevents motility and the invasion of hepatocellular carcinoma (HCC) cells^[17].

However, our previous work found that although CD147 expression is maintained at a high level, its expression level varies across different cancer types. The correlation between CD147 expression level and the degree of tumor development is unclear. Furthermore, most reports show that CD147 tends to be more widely involved in tumor invasion and cell motility^[18,19]. Nevertheless, its involvement in the

maintenance of tumor proliferation and apoptosis resistance has rarely been reported, and its specific mechanism requires further elucidation. Moreover, AC-73 has several limitations as a potential preclinical candidate compound (PCC). One of the most urgent problems is that AC-73 mainly inhibits cancer invasion rather than cancer cell viability and proliferation. Therefore, AC-73 may only affect terminal-stage tumors with no obvious effects on early-stage tumors.

In the present work, we first verified a significant correlation between CD147 expression level and cancer cell viability. We then synthesized a novel compound, HA-08 (China Patent ZL 2015 10790209.7), which was demonstrated to be more active than AC-73. Further functional tests were performed to evaluate the anticancer properties of HA-08, which included inhibition of cancer cell proliferation and promotion of apoptosis both *in vitro* and *in vivo*. Finally, the underlying molecular mechanisms of HA-08 were explored. In summary, our research clarified the important role of CD147 in promoting tumor proliferation and apoptosis resistance. Additionally, the novel anticancer compound HA-08 may provide a new strategy for the treatment of tumors.

METHODS

Reagents

An antibody against CD147 (mAb HAb18) was prepared by our lab. Antibodies against α -tubulin (sc-8035) were purchased from Santa Cruz (Dallas, TX). Primary antibodies against p-ERK, PARP, Bcl-2, Bcl-xl, and Bak were obtained from Cell Signaling Technology. The Caspase inhibitor Z-VAD-FMK was purchased from R&D Systems. Dyes of Hoechst 33258 and JC-1 were brought from Sigma.

Cell Lines and Cell Culture

Three lung cancer cell lines NCI-H460, NCI-H1299, and NCI-H292 were purchased from the Shanghai Institutes for Biological Sciences (Shanghai, China). U-87, A-431, SK-BR-3, MDA-MB-231, MCF-7, and MIA-PaCa-2 cell lines were obtained from the American Type Culture Collection (ATCC; Manassas, VA, USA). The HCC cell lines SMMC-7721 (7721) and Huh-7 were purchased from the Institute of Cell Biology of Academia Sinica (Shanghai, China) and the Cell Bank of the JCRB (Tokyo, Japan), respectively. The colon cancer cell line Hct-8 and Chinese hamster ovarian cell line CHO were brought from the

Shanghai Life Sciences Institute. All cells were authenticated by short tandem repeat profiling. The cells were cultured in DMEM supplemented with 10% FBS, 1% penicillin/streptomycin, and 2% L-glutamine at 37 °C in a humidified atmosphere of 5% CO₂.

Synthesis of HA-08

Synthesis of N-(4-bromobenzyl)-2-(3-hydroxyphenyl) acetamide: 4-Bromobenzylamine hydrochloride (1.335 g, 6 mmol), N-(3-dimethylaminopropyl)-N'-ethylcarbodiimide hydrochloride (0.69 g, 3.6 mmol), 1-hydroxybenzotriazole (0.487 g, 3.6 mmol), and triethylamine (1.212 g, 12 mmol) were dissolved in dichloromethane and 3-hydroxyphenylacetic acid was added in two batches with an interval of 15 min. The resulting mixture was stirred at room temperature for 8 h. The reaction was then diluted with dichloromethane and washed with 0.5 N hydrochloric acid, water and brine, dried over anhydrous sodium sulfate, filtered, and concentrated to give a crude product N-(4-bromobenzyl)-2-(3-hydroxyphenyl) acetamide 0.96 g, which was used without further treatment. MS (ESI): 320.3(M+H).

Synthesis of N-[(1,1'-biphenyl)-4-ylmethyl]-2-(3-hydroxyphenyl) acetamide: N-(4-bromobenzyl)-2-(3-hydroxyphenyl) acetamide (0.96 g, 3 mmol), Phenylboronic Acid (0.367 g, 3 mmol), and a palladium catalyst (0.049 g, 0.06 mmol) were dissolved in methylbenzene and 3 mL of a 2 mol/L sodium carbonate aqueous solution was added. The reaction mixture was reflux stirred for 2 h under nitrogen, and then cooled to room temperature. The reaction was then diluted with ethyl acetate and acidified with 1 N hydrochloric acid to a pH of 4 and washed with water and brine, dried over anhydrous sodium sulfate, filtered and concentrated to give a crude product. The crude product was purified on silica gel, eluted with a gradient of petroleum ether: acetone = 4:1 to 3:1 to give N-[(1,1'-biphenyl)-4-ylmethyl]-2-(3-hydroxyphenyl) acetamide 0.476 g. ¹H NMR (400 MHz, DMSO-*d*₆): δ 9.32 (d, *J* = 2.1 Hz, 1H), 8.55 (t, *J* = 6.0 Hz, 1H), 7.67-7.57 (m, 4H), 7.50-7.41 (m, 2H), 7.39-7.28 (m, 3H), 7.13-7.04 (m, 1H), 6.74-6.59 (m, 3H), 4.34-4.25 (m, 2H), 3.41-3.37 (m, 2H), MS (ESI): 318.3 (M+H).

Synthesis of 3-(2-([(1, 1'-biphenyl]-4-ylmethyl) amino) ethyl) phenol: To a stirred solution of N-[(1,1'-biphenyl)-4-ylmethyl]-2-(3-hydroxyphenyl) acetamide (0.476 g, 1.5 mmol) and sodium borohydride (0.143, 3.75 mmol) in dry

tetrahydrofuran (THF) at -10 °C. A solution of iodine (0.381 g, 1.5 mmol) in dry THF was added drop by drop, at a slow and controlled rate. The resulting mixture was warmed to reflux stirring for 3 h and then cooled to 10 °C. The reaction solution was adjusted with 1N NaOH to a pH > 10 and then extracted with ethyl acetate. The combined organic layer was washed with water and brine, and dried over anhydrous sodium sulfate. The solvent was evaporated under reduced pressure and the residue was chromatographed over silica gel eluting with petroleum ether: acetone = 1:1 containing 0.5% triethylamine to yield 0.40 g (87%). ¹H NMR (400 MHz, DMSO-*d*₆): δ 9.23 (s, 1H), 7.69–7.55 (m, 5H), 7.49–7.31 (m, 5H), 7.04 (t, *J* = 7.7 Hz, 1H), 6.65-6.52 (m, 3H), 3.74 (s, 2H), 2.67 (dd, *J* = 15.5, 6.3 Hz, 4H), ¹³C NMR (101 MHz, DMSO): δ 157.66, 142.27, 140.66, 140.51, 138.81, 129.56, 129.31, 128.92, 127.63, 126.95, 126.82, 119.63, 115.85, 113.20, 52.92, 50.84, 36.33, MS (ESI): 304.3 (M+H).

Cell Viability Assay

Specifically, all types of cells were first seeded in 96-well plates (5.0 × 10³ cells/well) with 100 μL media and incubated at 37 °C overnight with various concentrations of HA-08 (0, 5, 10, 20, 40, 60 μmol/L) for 48 h. After incubation, 10 μL WST-1 reagent was added to each well, and the cells were incubated at 37 °C for 2 h. The plates were read on a microplate reader (OD450) after being shaken thoroughly.

Flow Cytometry Analysis

Cancer cells were treated with different concentrations of HA-08. After 48 h, the cells were harvested by centrifugation and washed twice in PBS. Apoptosis was measured by flow cytometry (BD FACS Calibur) with the FITC and DAPI channels after staining with fluorescein isothiocyanate (FITC)-conjugated Annexin V (AV, 5:100, V:V) and propidium iodide (PI, 5 mg/mL) as described in the FITC Annexin V Apoptosis Detection Kit II manual (BD Biosciences). The total number of Annexin V positive cells was recorded for further analysis.

Hoechst 33258 Staining

To examine whether HA-08 induces apoptosis in two lung cancer cell lines, NCI-H1299 and A549, cells were plated in six-well plates, and treated with 0, 30, 60 μmol/L of HA-08 for 48 h. For Hoechst 33258 staining, cells were washed with PBS and fixed for 10 min at room temperature. The cells were then rinsed twice with PBS and stained with Hoechst 33258 fluorescent dye, at room temperature in the dark for

10 min. After being washed twice with PBS, the cells were examined and immediately photographed under a fluorescence microscope with an excitation wavelength of 330-380 nm. Apoptotic cells were defined based on nuclear morphology changes such as chromatin condensation and fragmentation.

Measurement of Mitochondrial Membrane Potential

Cells treated with 0, 5, 30 $\mu\text{mol/L}$ of HA-08 for 48 hrs. were incubated with 5 mg/mL JC-1 for 20 min at 37 °C and examined with fluorescence microscopy. The emission fluorescence for JC-1 was monitored at 530 and 590 nm, with an excitation wavelength of 488 nm. The orange-red emission of the dye is attributable to potential dependent aggregation in the mitochondria, which reflects the $\Delta\phi$. Green fluorescence reflects the monomeric form of JC-1, appearing in the cytosol after mitochondrial membrane depolarization.

In Vivo Antitumor Efficacy Studies

To determine the *in vivo* anti-cancer activity of HA-08, viable human lung cancer cells (10^6 A549 cells) were subcutaneously injected into the right flank of 4-6-week-old Balb/c nude mice. Two weeks after infection, mice were randomly divided into five groups (five mice per group): vehicle group, low concentration group, medium concentration group, high concentration group, and high concentration without xenograft group. Tumor size was measured every two days with a caliper (calculated volume = shortest diameter² \times longest diameter/2). Body weight, diet consumption, and tumor size were also recorded every two days. After four weeks, the mice were sacrificed and their tumors were excised and weighed before being stored at -80 °C until further analysis.

Western Blot Analysis

Cancer cells were suspended in serum-free media in a six-well plate at a density of $2.5 \times 10^5/\text{mL}$. A 2 mL of cell suspension, containing different concentrations of HA-08 were used. After cell attachment, the conditioned media was collected. Tumor samples were minced on ice in pre-chilled lysis buffer containing phenylmethylsulfonyl fluoride, protease inhibitors, and phosphatase inhibitors (KeyGen BioTech, China). Homogenized tissues and cell lysates were then centrifuged at 14,000 rpm at 4 °C for 15 min. A BCA Protein Assay Kit (Pierce Biotechnology, Rockford, IL) was used to determine the total protein density and to ensure that equal amounts of proteins were separated on the 10% SDS

PAGE gel and transferred to a polyvinylidene fluoride (PVDF) membrane (Millipore, Boston, MA). After blocking with 5% nonfat milk for 1 hrs. the membrane was incubated with the designated primary antibody at 4 °C overnight. Immunodetection was performed using a Western-Light chemiluminescent detection system (Applied Biosystems, Foster City, CA) after incubation with the secondary antibody for 1 h.

Statistical Analysis

Statistics were evaluated using GraphPad Prism V5.0 software (GraphPad Software, La Jolla, CA). Each experiment was repeated at least three times. Statistical analysis was carried out using one-way ANOVA (multiple comparisons) and Student's *t*-test (two comparisons, or two tailed). Differences were deemed significant if $P < 0.05$. (** indicates $P < 0.001$, * indicates $P < 0.01$, # indicates $P < 0.05$, and # indicates $P > 0.05$ in Figures). IC50 ($\mu\text{mol/L}$) 95% confidence intervals were analyzed by nonlinear regression (curve fit) in the GraphPad Prism 5.0 software package.

RESULTS

A Positive Correlation Exists between CD147 Expression and of Tumor Cell Proliferation

To evaluate whether CD147 expression affects cancer cell proliferation, we used 3 human cancer cell lines with different CD147 expression levels. Using real-time PCR and Western blot assays, we confirmed that CD147 was relatively highly expressed in U-87 cells, moderately expressed in A-431 cells, and poorly expressed in SK-BR-3 cells at both the mRNA and protein levels (Figure 1A and 1B). Interestingly, using a WST-1 assay, we found that U-87 cells exhibited the highest proliferative activity. Within 24 hours, the level of proliferation by U-87 cells was 60%, that of A-431 cells was 40% and that of SK-BR-3 cells was 20%. Thus, there is a possibility that in these tumor cells, higher CD147 expression causes stronger proliferative activity (Figure 1C). To further test this finding, a parallel test was performed using two other lung cancer cell lines: NCI-H460 (460) and NCI-H1299 (1299). A previous study demonstrated that CD147 exhibits higher expression levels in 460 cells than in 1299 cells^[20]. Using WST-1 assays, we also verified that the viability of 460 cells was much greater than that of 1,299 cells under intervention with cisplatin, a broad-spectrum antineoplastic drug (Figure 1D).

Furthermore, we altered the expression level of CD147 in each lung cancer cell line and compared proliferation (Figure 1E). As shown in Figure 1F and 1G, using the same drugs (cisplatin), we observed that proliferation was reduced in NCI-H460 cells, in

which CD147 was knocked down (460 CD147-), but was increased in NCI-H1299 cells, where CD147 was overexpressed (1299 CD147+). In summary, we showed a positive correlation between CD147 expression and tumor cell proliferation.

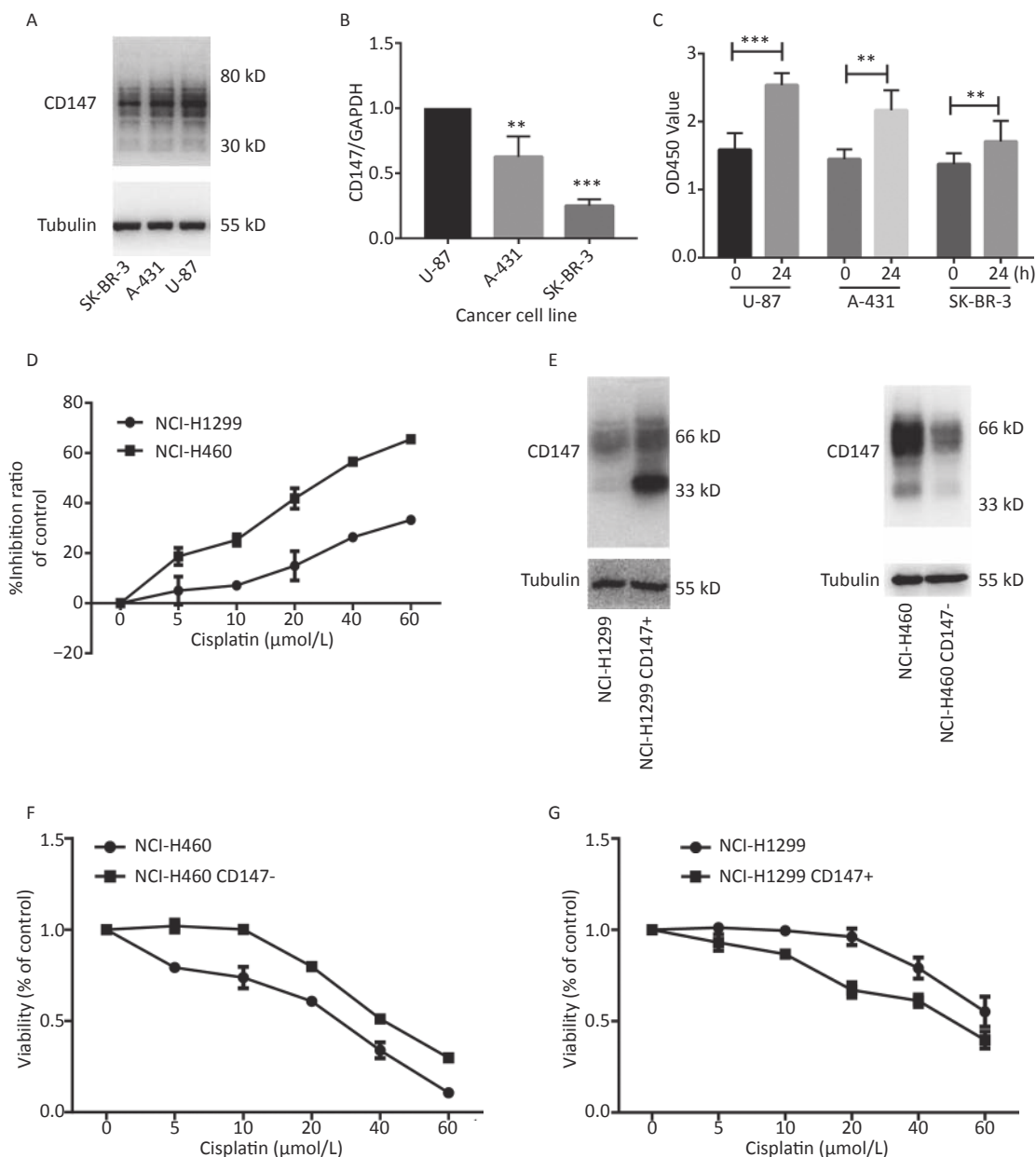


Figure 1. Positive correlation between the level of CD147 expression and cancer cell viability. (A) Expression of CD147 in various cancer cell lines at the protein level; (B) Expression of CD147 in various cancer cell lines at the mRNA level. (C) Proliferation of cell lines as measured by WST-1 assays; (D) Inhibitory effects of antitumor drugs on cell viability in NCI-H460 and NCI-H1299 cells; (E) Changes in the expression level of CD147 in each lung cancer cell line; (F and G) Effect of drugs on cell viability with changes in the expression level of CD147 in each lung cancer cell line measured by aWST-1 assay. All the bars represent the mean of three measurements for each sample, and the error bars indicate \pm SD. *** $P < 0.001$, ** $P < 0.01$, Student's *t*-test.

The Novel Compound HA-08 Synthesized Based on AC-73 Exhibits Better Antitumor Activity

Our previous work identified a novel compound (AC-73) that could significantly inhibit cancer invasion in HCC by targeting CD147. However, AC-73 barely reduced cancer cell proliferation at certain concentrations^[17]. Therefore, we synthesized another compound, HA-08 (Figure 2A), based on the structure of AC-73. To evaluate whether HA-08 is more active than AC-3, a WST-1 assay was performed to assess their tumor inhibitory activity. HA-08 exhibited better anticancer properties than AC-73 on Huh-7 cells treated with the same concentration (Figure 2B). A Western blot assay was used to examine the effects of both compounds on the expression of proliferation- and apoptosis-related proteins in Huh-7 cells. As shown in Figure 2C, we observed that HA-08 had a greater effect on the expression of ERK1/2, Bcl-2, and Bak than AC-73. In fact, HA-08 also exerted greater cytotoxicity on other cancer cell lines (Figure 2D-2J). These results suggested that, compared with AC-73, the new compound, HA-08, was better in terms of tumor suppressor activity and promoting apoptosis.

HA-08 Inhibits Cancer Cell Viability

We next assessed the effect of HA-08 on cell viability in human cancer cell lines other than HCC. As shown in Table 1, ten cancer cell lines in total were treated with HA-08 for 48 h and then subjected to a WST-1 assay. The anticancer activity of HA-08 was quantified by determining the IC₅₀ values, which were found to be in the micromolar range. In general, HA-08 could effectively reduce the viability of many types of human cancer cells (breast cancer cell lines, non-small cell lung cancer (NSCLC) cell lines, pancreatic cancer cell lines and colorectal cancer cell lines), but not Chinese hamster ovary (CHO) cells. Specifically, MDA-MB-231, NCI-H460, and A549 cells appeared to have relatively high sensitivity to HA-08, with IC₅₀ values below 30 μmol/L. Huh-7, NCI-H1299, NCI-H292, and MIA-PaCa-2 cells had relatively moderate sensitivity to HA-08, with IC₅₀ values between 30 μmol/L and 50 μmol/L. MCF-7 and HCT-8 cells had relatively low sensitivity to HA-08, with IC₅₀ values from 60 μmol/L to 100 μmol/L. Finally, the CHO cell line was essentially resistant to HA-08 (IC₅₀ > 100 μmol/L). From these results, we can conclude that compared to AC-73, HA-08 is more cytotoxic to human malignant cell lines but less cytotoxic to normal cells.

HA-08 Induces Cancer Cell Apoptosis

To determine whether HA-08 induces malignant cell death, we chose two cancer cell lines, MDA-MB-231 and NCI-H1299, which exhibited relatively high sensitivity and moderate sensitivity to HA-08, respectively. The number of apoptotic cells after treatment with HA-08 was determined by positive annexin V staining, marks phosphatidylserines on the surface of apoptotic cells (Figure 3A-3D). We observed that both cancer cell lines underwent apoptosis after exposure to HA-08 in a dose-dependent manner, although higher concentrations were required for NCI-H1299 cells than for MDA-MB-231 cells. To determine whether caspases are involved in HA-08-induced apoptosis, we measured the level of apoptosis with or without the caspase inhibitor Z-VAD-FMK (ZVAD) in A549 cells, which have relatively high sensitivity to HA-08. The results indicated that ZVAD significantly reduced the degree of HA-08-induced apoptosis (Figure 3E and 3F), suggesting that HA-08 induces apoptosis mainly through a caspase-dependent pathway. However, some contribution by a caspase-independent pathway cannot be excluded.

Next, we morphologically characterized apoptotic cells in two lung cancer cell lines using Hoechst 33258 staining. A549 and NCI-H1299 cells were treated with or without HA-08 and their nuclei were stained with Hoechst 33258 to detect apoptotic morphology. In the control groups, the nuclei of both cell types had regular, round contours. In contrast, the nuclei of cells treated with HA-08 appeared to undergo chromatin condensation and nuclear fragmentation in a dose-dependent manner, both of which are typical hallmarks of apoptosis (Figure 4A). In addition, changes in the mitochondrial membrane potential of three different malignant cell lines were detected using JC-1 staining. JC-1 molecules localize to the mitochondrial matrix in the cytosol and form J-aggregates in nonapoptotic cells, which emit orange fluorescence. In apoptotic cells, JC-1 molecules exist in a monomeric form, and the cytosol emits green fluorescence. In Figure 4B, we observed that with JC-1 staining, the cytosolic emission transitioned from orange to green with increasing concentrations of HA-08. Interestingly, the three cell lines did not show a significantly different sensitivity to HA-08, and HCT-8 cells showed relatively low sensitivity to HA-08-induced inhibition of cell viability. This indicated that HA-08 increases cancer cell apoptosis by destroying the permeability of mitochondrial membranes and

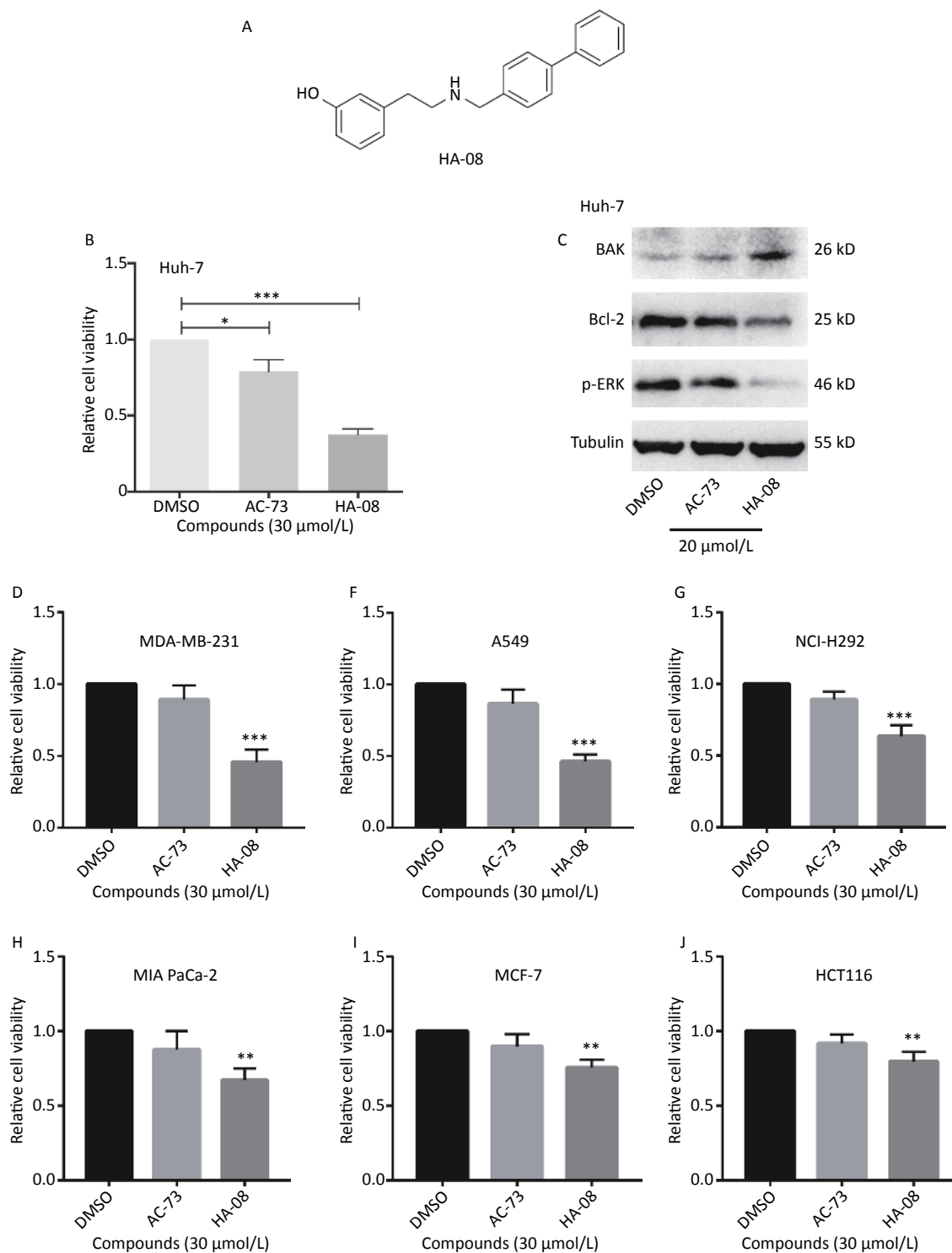


Figure 2. HA-08 exhibits better antitumor activity than AC-73. (A) Substituent structure of HA-08; (B, D-J) Differences in cell viability under exposure to AC-73 and HA-08 measured by WST-1 assays; (C) Effects of both compounds on the expression of proliferation- and apoptosis-related proteins in cancer cells as measured by Western blot assays. All the bars represent the mean of three measurements of each sample, and the error bars indicate \pm SD. *** $P < 0.001$, ** $P < 0.01$, * $P < 0.05$, one-way ANOVA (H) for multiple comparisons.

altering their potential.

Next, we determined the expression levels of apoptosis-regulating proteins in both A549 and NCI-H460 cells after exposure to HA-08 (0, 10, 20, or 30 $\mu\text{mol/L}$). These results showed that HA-08 significantly reduces expression of Bcl-2 and Bcl-xL, which are antiapoptotic molecules. Moreover, the expression of BAK, which is part of a family of proapoptotic factors, was increased after HA-08 treatment. Furthermore, we found that poly (ADP-ribose) polymerase (PARP) cleavage was activated by HA-08 in a dose-dependent manner, which is a sign of cell apoptosis (Figure 4C). Taken together, our results suggested that HA-08 plays a vital role in promoting cancer cell apoptosis.

HA-08 Inhibits Tumor Viability *in Vivo*

In addition to results from *in vitro* assays, we examined whether HA-08 could inhibit tumor growth in xenografts in nude mice. A549 cells were prepared and injected into the right back side of nude mice. After cell injection, the mice were randomly divided into 5 groups and given different concentrations of HA-08. The weight of the mice was continuously monitored for 4 weeks; the mice were then sacrificed, and the subcutaneous transplanted tumors appeared to be striped, as shown in Figure 5A and 5B. We observed that HA-08 not only prevented tumor growth but also induced tumor death in a dose-dependent manner, based on calculations of tumor size, especially when the concentration of HA-08 reached 60 mg/kg (Figure 5C, 5D, and 5F). We found that over 4 weeks, the HA-08-treated groups generally exhibited a good condition, with a weight loss of less than 10% that of

the control group, even in the final group, which consisted of normal nude mice without xenografts treated with 60 mg/kg HA-08 (Figure 5E). This indicated that the HA-08 treatment resulted in no major toxicity or harm to the animals. Therefore, we suggest that HA-08 has potential therapeutic effects on the prevention of tumor growth.

HA-08 Induces Cancer Apoptosis Mainly by Reducing Bcl-2 Production through Blocking CD147-CD44 Stimulated JAK/STAT3 Signaling

In the final part of this study, we explored possible molecular signaling mechanisms of HA-08. As a candidate compound, HA-08 was first evaluated to be a protein-protein interaction inhibitor. Using a co-ip assay, we detected whether HA-08 could affect the interaction of CD147-HOOK1, CD147-RAP2, CD147-MCT4, and CD147-CD44, pairs of membrane proteins have been reported to clearly interact, initiating downstream signaling pathways, and are involved various biological process of cancer^[21-24]. The results showed that HA-08 barely affected the interaction of CD147-HOOK1, CD147-RAP2, and CD147-MCT4. However, HA-08 did disrupt the interaction of CD147 and CD44 in a dose dependent manner (Figure 6A and 6B). To further verify how HA-08 affects the interaction between the two proteins, immunofluorescence staining was performed. As shown in Figure 6C, we noticed that co-localization of CD147 and CD44 on cancer cell membrane was significantly disrupted with the exposure of HA-08 (10 $\mu\text{mol/L}$) compared to the control group (HA-08 0 $\mu\text{mol/L}$). Based on the above, we speculated that HA-08 inhibited the downstream signal pathways activated by the interaction

Table 1. Characteristics of cell lines screened by HA-08

Characteristics	Cell lines	Cell type	IC50 ($\mu\text{mol/L}$) 95% confidence intervals
Relatively high sensitivity ($\text{IC}_{50} < 30 \mu\text{mol/L}$)	MDA-MB-231	Breast, metastatic-pleural, invasive ductal carcinoma	26.47 \pm 1.04
	NCI-H460	Large cell lung cancer	21.08 \pm 1.06
	A549	Non-small cell lung cancer	29.57 \pm 1.1
Relatively Moderate sensitivity ($30 < \text{IC}_{50} < 50 \mu\text{mol/L}$)	Huh7	Hepatocellular carcinoma	36.19 \pm 1.05
	NCI-H1299	Non-small cell lung cancer	37.62 \pm 1.04
	NCI-H292	Non-small cell lung cancer	42.13 \pm 1.04
	MIA PaCa-2	Pancreatic carcinoma	42.43 \pm 1.02
Relatively Low sensitivity ($60 < \text{IC}_{50} < 100 \mu\text{mol/L}$)	MCF7	Breast, metastatic-pleural, invasive ductal carcinoma	60.50 \pm 2.31
	HCT116	Colorectal carcinoma	67.57 \pm 0.33
Resistant ($\text{IC}_{50} > 100 \mu\text{mol/L}$)	CHO	Cells from the ovaries of Chinese hamsters	> 100

between CD147 and CD44 through affecting their co-localization on the cancer cell membrane, thereby preventing their interaction. Next, we wondered which downstream signaling pathway of CD147-CD44 was mainly affected by HA-08. Our previous results indicated that HA-08 could be involved cancer apoptosis, including changing the expression of apoptosis-related molecules, such as the Bcl

family (Bcl-2, Bcl-xl). It has also been reported that CD147, interacting with CD44s, plays a critical role in the development of cancer, with high co-expression of CD147-CD44 being associated with grave apoptosis resistance and poor patient survival^[24,25]. In addition, as an important transcription factor in cancer cells, STAT3, a downstream molecule of CD147-CD44, is known to participate in tumor cell

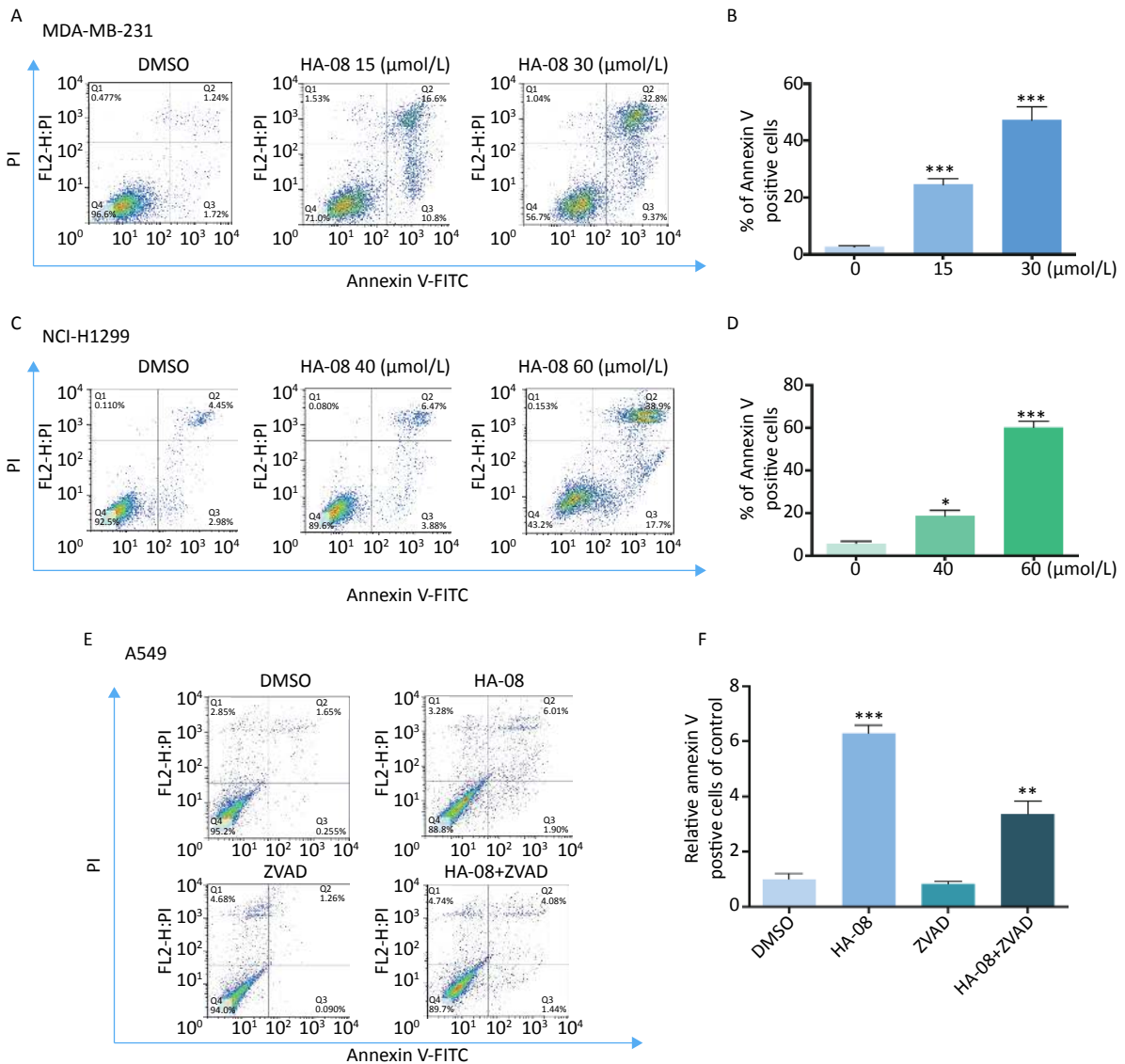


Figure 3. Effects of HA-08 on apoptosis determined by FACS analysis. Cells were left untreated or were treated with HA-08, and apoptosis was evaluated by FACS analysis after double cell labeling with propidium iodide (PI) and annexin V-FITC. (A) HA-08 (0, 15, 30 µmol/L) induces apoptosis in MDA-MB-231 cells; (B) Quantitative analysis of % annexin V-positive cells; (C) HA-08 (0, 40, 60 µmol/L) induces apoptosis in NCI-H1299 cells; (D) Quantitative analysis of % annexin V-positive cells; (E) Effect of HA-08 and ZVAD on apoptosis in A549 cells; (F) Quantitative analysis of % annexin V-positive cells. All the bars represent the mean of three measurements of each sample, and the error bars indicate ± SD. *** $P < 0.001$, ** $P < 0.01$, * $P < 0.05$, one-way ANOVA (H) for multiple comparisons (B, D, and E).

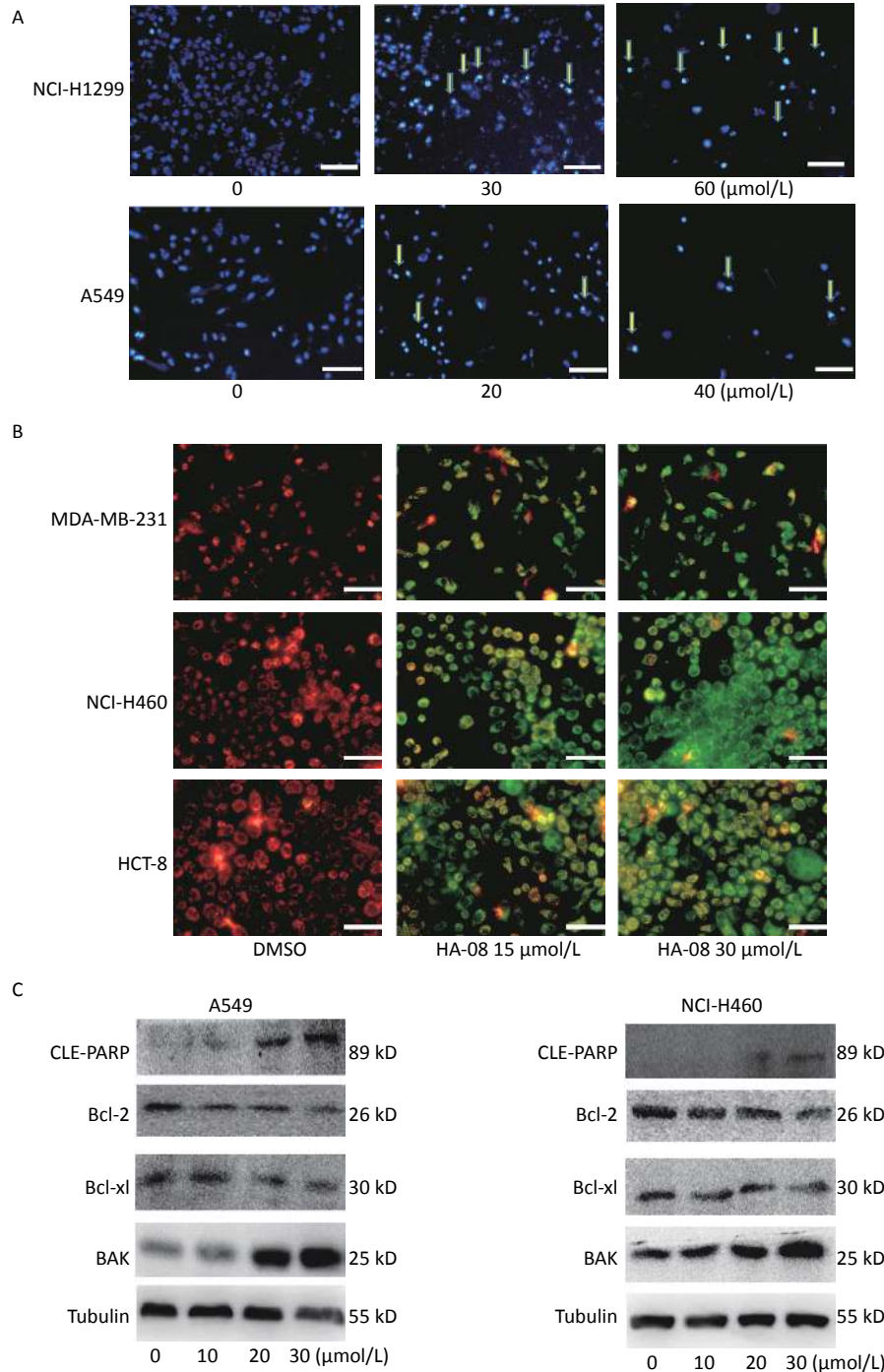


Figure 4. Effects of HA-08 on apoptosis based on morphological and molecular expression changes. (A) Morphological changes in the nuclei (typical of apoptosis) of lung cancer cell lines treated with HA-08 at various concentrations and stained with Hoechst 33258. Selected fields exhibiting condensed chromatin (yellow arrowhead) indicating the occurrence of cell apoptosis are shown. Each inset shows images at 100 \times magnification, scale bars: 100 μm ; (B) Collapse of the mitochondrial membrane potential of three cancer cell lines treated with 0, 15, or 30 $\mu\text{mol/L}$ HA-08 and stained with JC-1. Selected fields containing the corresponding live cells (orange-red) and apoptotic cells (green). Each inset shows images obtained at 100 \times magnification, scale bars: 100 μm ; (C) Western blot to determine the expression of apoptosis-related proteins in two lung cancer cell lines treated with different concentrations of HA-08.

apoptosis, when activated under the regulation of JAK^[26]. Therefore, we hypothesized that HA-08 induced cancer apoptosis by disrupting CD147-CD44 interaction and reducing downstream JAK/STAT3/Bcl-2 signaling. Using western blot assays, we detected the expression of signaling molecules in A549 cells with or without HA-08 (Figure 6D and 6E). HA-08 was found not to change the protein expression of JAK and STAT3. However, the phosphorylation of JAK and STAT3 was suppressed in a dose dependent manner after treatment with HA-08 for 6 hrs. Further, through examination of tissue pathology in original orthotopic tumors, we found that HA-08 inhibited

Bcl-2 expression through down-regulating the phosphorylation of JAK and STAT3 in a dose dependent manner (Figure 6F and 6G), suggesting that HA-08 suppresses the JAK/STAT3/Bcl-2 pathway *in vivo*. To sum up, HA-08 induced cancer apoptosis mainly by disrupting CD147-CD44 interaction and reducing downstream JAK/STAT3/Bcl-2 signaling.

DISCUSSION

In this study, we determined that the expression level of CD147 in different tumor cell lines was positively correlated with cell proliferation. On this basis, we synthesized a new small-molecule

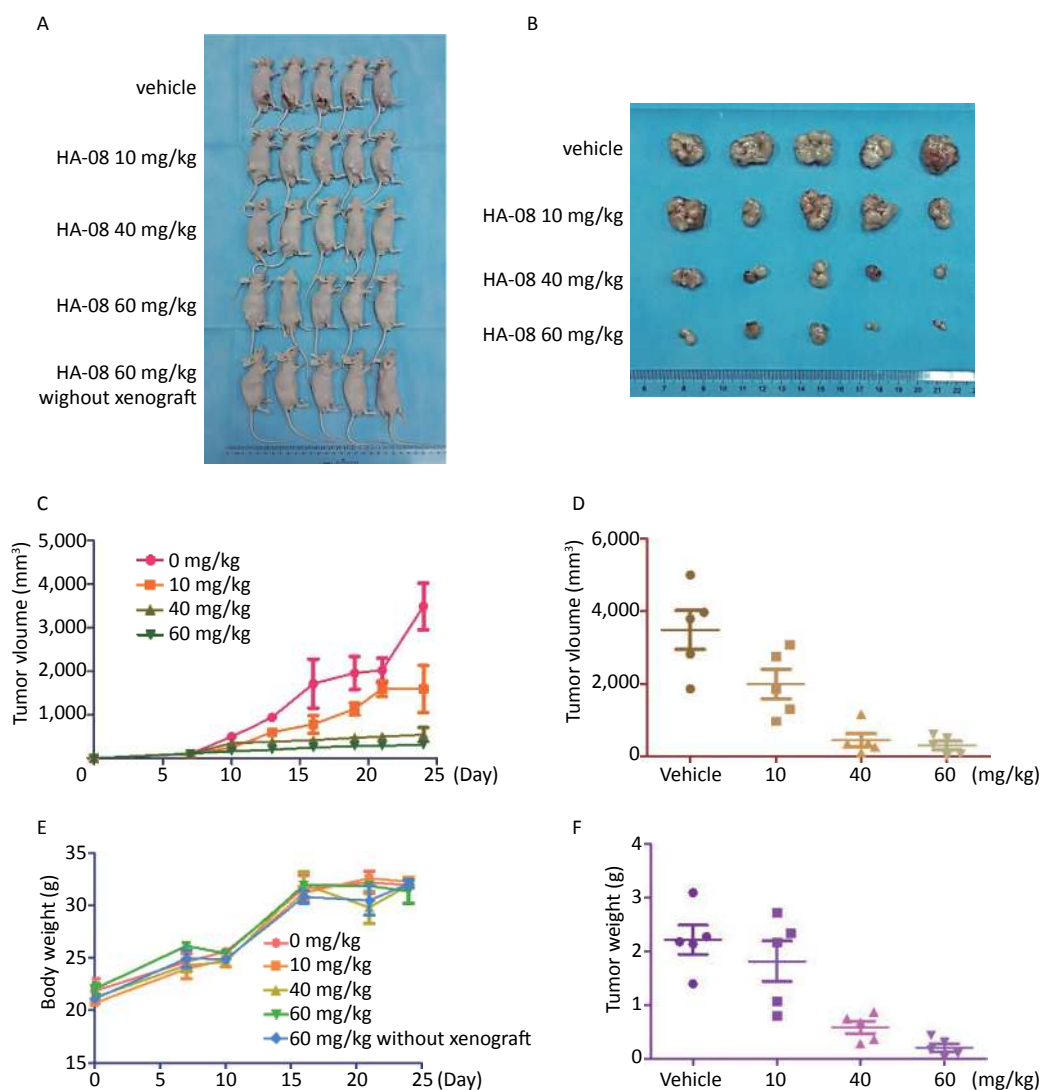


Figure 5. HA-08 inhibits A549 cell tumorigenesis in a xenograft model. Tumor-bearing mice were treated intravenously with the vehicle or HA-08 (10, 40, and 60 mg/kg). (A and B) Gross anatomy of nude mice and exfoliated tumor tissue; (C and D) Tumor size; (E) Body weight; (F) Tumor weight. Data are presented as the mean \pm SD.

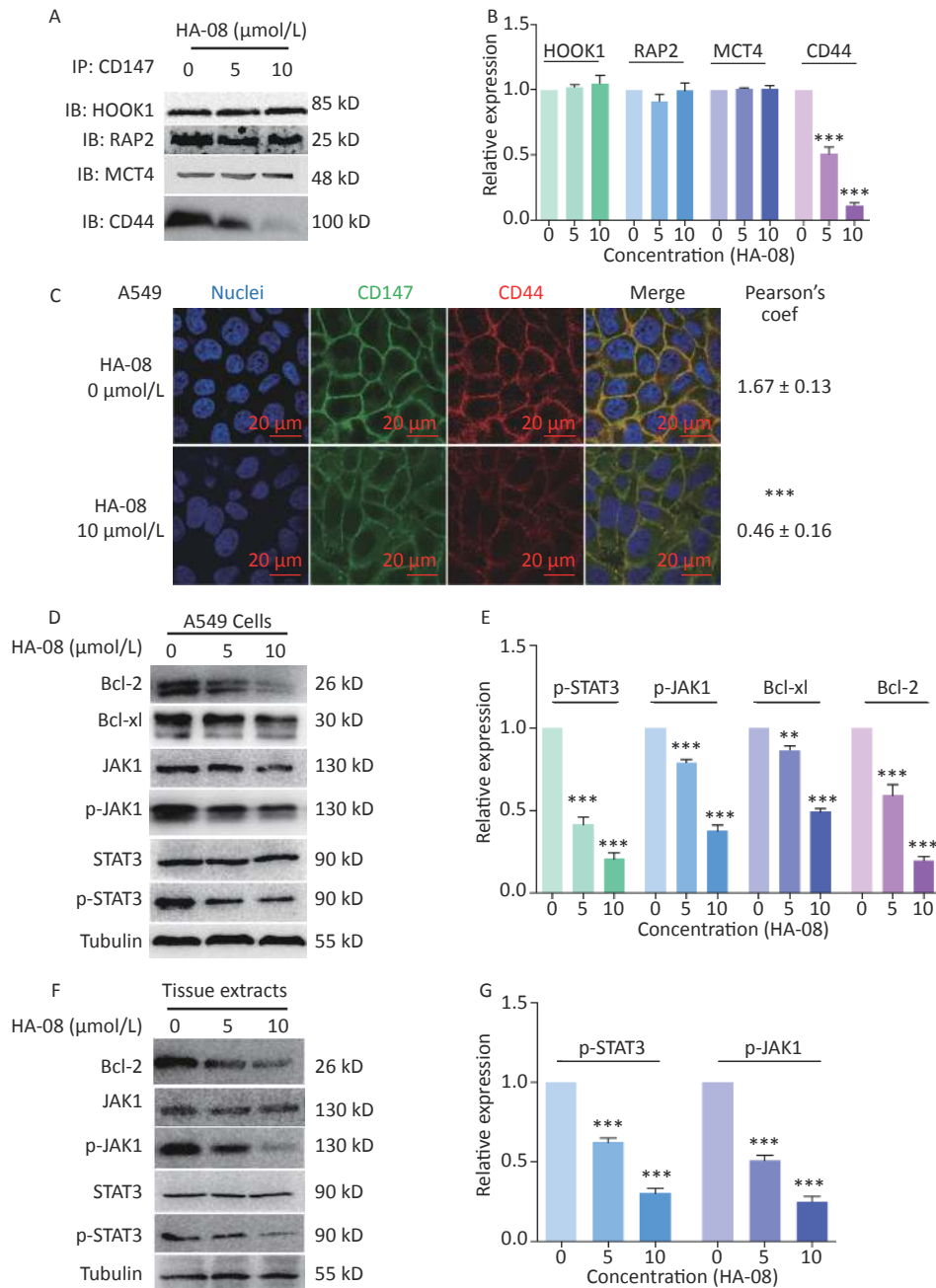


Figure 6. Molecular mechanism of action of HA-8 in cancer cells. (A) Representative image of Co-IP analysis between CD147 and related proteins. HA-8 blocks CD147-CD44 interaction. (B) Quantification of protein expression by densitometry analysis. (C) Co-localization of CD147 and CD44 in A549 cells. Cells (5×10^5) were grown on coverslips for 24 h, fixed, and stained with Dylight488-conjugated goat-anti-mouse antibodies (CD147, green) and Dylight594-conjugated goat-anti-rabbit antibodies (CD44, red; Pearson's coefficients are indicated as numerical data to the right of each panel, $n = 3$). Bar, 20 μm. (D, E) Bcl-2, Bcl-xl, JAK, and STAT3 activities and total JAK and STAT3 expression in A549 cells treated with different concentrations of HA-8. (F, G) Phosphorylation of JAK and STAT3 in total lysates of original orthotopic tumors from each group. The histogram shows quantification of the gray scale analysis from western blotting. All the Histograms show quantification of the gray scale analysis from western blotting. The bars represent the mean of each sample measured in triplicate and the error bars indicate \pm SD. (***) $P < 0.001$, (**) $P < 0.01$, one-way ANOVA (H) for multiple comparisons.

compound (HA-08) that is more active than AC-73. We confirmed that it can inhibit cancer viability and induce cancer cell apoptosis both *in vitro* and *in vivo*. We hypothesized that HA-08 reduces CD147-CD44 interaction which leads to lower Bcl-2 production, apparently through suppression of the JAK/STAT3 signaling pathway.

As a potential tumor-specific molecule, CD147 has been reported to be overexpressed in many types of cancers and is involved in many of the hallmarks of cancer, as described by Weinberg RA et al.^[27]. Earlier studies have focused on the characteristics of CD147 promoting cancer cell motility and invasion^[28]. The primary mechanisms of CD147 include inducing MMPs, inducing CD147-CD147 dimerization, and upregulating metastasis-related genes (FAK, STAT3, etc.)^[29-33]. Until recently, literature reports have shown that CD147 could mediate sustained proliferative signaling and resistance to cell death in lung cancer, breast cancer, and pancreatic cancer *via* different molecular mechanisms^[12,15,34]. Our study confirmed that higher CD147 expression is correlated with increased cell proliferation, by comparing cell lines with different CD147 expression levels and by altering CD147 expression in the same cell lines. Moreover, the functional characteristics of CD147 as a tumor-specific molecule were further verified. In addition, our findings provide a theoretical basis for screening tumor suppressor drugs that target this protein.

To date, among all drugs targeting CD147, only the second generation humanized mAb matuzumab has been reported to inhibit lung cancer cell proliferation to a relevant extent^[35,36]. Nevertheless, its anticancer activity mostly depends on antibody-dependent cell-mediated cytotoxicity (ADCC) rather than on the target itself. Therefore, to our knowledge, HA-08 is the first compound to inhibit cancer cell viability and induce cell death by targeting CD147. Structurally, the unique chiral group in AC-73 was replaced with hydrogen, which made HA-08 easy to synthesize and purify. Functionally, AC-73 was ineffective at killing cancer cells, indicating that it could not treat tumors effectively. HA-08 inhibited cancer cell viability and proliferation, suggesting that it might be effective at intervening in cancer progression at an early stage.

In addition to CD147, important target molecules were found to be involved in the cancer-specific characteristics of self-sufficient growth signals and resistance to cell death. Small-molecule drugs targeting these molecules were also efficacious in both clinical and preclinical studies. For instance,

mitogen-activated protein kinase (MAPK) and tyrosine kinases were initially recognized as cancer targets, and several inhibitors of these kinases, such as Gefitinib, Vemurafenib, and Dabrafenib among others, have been approved by the FDA for cancer treatment due to their ability to inhibit cancer cell proliferation^[37-41]. ABT-199, ABT-737, olaparib, and iniparib have been reported to be potent candidate drugs due to their ability to induce cancer cell death by targeting the apoptosis-regulating proteins Bcl-2 or PARP^[42-46]. Based on comparisons with these drugs, HA-08 should be further modified to enhance its anticancer effects, since for small-molecule compounds structure is the basis of function. Some key synthetic steps and structural modifications may directly improve the anticancer activity of such compounds^[47,48]. Therefore, HA-08 needs to be modified.

CONCLUSION

Our study reveals a promising therapeutic application for HA-08. Discovery of this novel compound not only further emphasizes the drug target characteristics of CD147 but also provides a possible strategy for tumor therapy. Such an approach may have benefits as it could suppress cell viability and induce cancer cell apoptosis.

Received: June 4, 2019;

Accepted: July 25, 2019

REFERENCES

1. M Mesnil, T Aasen, J Boucher, A, et al. An update on minding the gap in cancer. *Biochim Biophys Acta*, 2018; 1860, 237–43.
2. RL Siegel, KD Miller, and A Jemal. Cancer Statistics, 2017. *CA Cancer J Clin*, 2017; 67, 7–30.
3. ST Chang, CO Menias, MG Lubner, et al. Molecular and Clinical Approach to Intra-abdominal Adverse Effects of Targeted Cancer Therapies. *Radiographics*, 2017; 1, 160–2.
4. JM Argiles, FJ Lopez-Soriano, B Stemmler, et al. Novel targeted therapies for cancer cachexia. *Biochem J*, 2017; 474, 2663–78.
5. V MacDonald. Chemotherapy: managing side effects and safe handling. *Can Vet J*, 2009; 50, 665–8.
6. A Roohi, M Hojjat-Farsangi. Recent advances in targeting mTOR signaling pathway using small molecule inhibitors. *J Drug Target*, 2017; 25, 189–201.
7. M Hojjat-Farsangi. Small-molecule inhibitors of the receptor tyrosine kinases: promising tools for targeted cancer therapies. *Int J Mol Sci*, 2014; 15, 13768–801.
8. GN Li, SP Wang, X Xue, et al. Monoclonal antibody-related drugs for cancer therapy. *Drug Discov Ther*, 2013; 7, 178–84.
9. DH Chen, XS Zhang. Targeted therapy: resistance and re-sensitization. *Chin J Cancer*, 2015; 34, 496–501.
10. C Biswas, Y Zhang, R DeCastro, et al. The human tumor cell-derived collagenase stimulatory factor (renamed EMMPRIN) is

- a member of the immunoglobulin superfamily. *Cancer Res*, 1995; 55, 434-9.
11. Y Li, J Xu, L Chen, et al. HAB18G (CD147), a cancer-associated biomarker and its role in cancer detection. *Histopathology*, 2009; 54, 677-87.
 12. YL Yong, CG Liao, D Wei, et al. CD147 overexpression promotes tumorigenicity in Chinese hamster ovary cells. *Cell Biol Int*, 2016; 40, 375-86.
 13. T Muramatsu. Basigin (CD147), a multifunctional transmembrane glycoprotein with various binding partners. *J Biochem*, 2015; 195, 481-90.
 14. L Xiong, C Edwards, L Zhou. The Biological Function and Clinical Utilization of CD147 in Human Diseases: A Review of the Current Scientific Literature. *Int J Mol Sci*, 2014; 15, 17411-41.
 15. X Xu, S Liu, B Lei, et al. Expression of HAB18G in non-small lung cancer and characterization of activation, migration, proliferation, and apoptosis in A549 cells following siRNA-induced downregulation of HAB18G. *Mol Cell Biochem*, 2013; 383, 1-11.
 16. I Marchiq, J Albregues, S Granja, et al. Knock out of the BASIGIN/CD147 chaperone of lactate/H⁺ symporters disproves its pro-tumour action via extracellular matrix metalloproteinases (MMPs) induction. *Oncotarget*, 2015; 6, 24636-48.
 17. ZG Fu, L Wang, HY Cui, et al. A novel small-molecule compound targeting CD147 inhibits the motility and invasion of hepatocellular carcinoma cells. *Oncotarget*, 2016; 7, 9429-47.
 18. J Xu, HY Xu, Q Zhang, et al. HAB18G/CD147 functions in invasion and metastasis of hepatocellular carcinoma. *Mol Cancer Res*, 2007; 5, 605-14.
 19. P Zhao, W Zhang, SJ Wang, et al. HAB18G/CD147 promotes cell motility by regulating annexin II-activated RhoA and Rac1 signaling pathways in hepatocellular carcinoma cells. *Hepatology*, 2011; 54, 2012-24.
 20. F Fei, X Li, L Xu, et al. CD147-CD98hc complex contributes to poor prognosis of non-small cell lung cancer patients through promoting cell proliferation via the PI3K/Akt signaling pathway. *Ann Surg Oncol*, 2014; 21, 4359-68.
 21. Maldonado-Baez L, Donaldson JG. Hook1, microtubules, and Rab22: mediators of selective sorting of clathrin-independent endocytic cargo proteins on endosomes. *Bioarchitecture*, 2013; 3, 141-6.
 22. Pereira-Vieira J, Azevedo-Silva J, Preto A, et al. MCT1, MCT4 and CD147 expression and 3-bromopyruvate toxicity in colorectal cancer cells are modulated by the extracellular conditions. *Biol Chem*, 2019; 400, 787-99.
 23. Zhang MY, Zhang Y, Wu XD, et al. Disrupting CD147-RAP2 interaction abrogates erythrocyte invasion by Plasmodium falciparum. *Blood*, 2018; 131, 1111-21.
 24. Li L, Tang W, Wu X, et al. HAB18G/CD147 promotes pSTAT3-mediated pancreatic cancer development via CD44s. *Clin Cancer Res*, 2013; 19, 6703-15.
 25. Grass GD, Tolliver LB, Bratoeva M, et al. CD147, CD44, and the epidermal growth factor receptor (EGFR) signaling pathway cooperate to regulate breast epithelial cell invasiveness. *J Biol Chem*, 2013; 288, 26089-104.
 26. Kondo R, Ishino K, Wada R, et al. Downregulation of protein disulfideisomerase A3 expression inhibits cell proliferation and induces apoptosis through STAT3 signaling in hepatocellular carcinoma. *Int J Oncol*, 2019; 54, 1409-21.
 27. D Hanahan, RA Weinberg. Hallmarks of cancer: the next generation. *Cell*, 2011; 144, 646-74.
 28. ZY Tang, L Ye, YK Liu, et al. A decade's studies on metastasis of hepatocellular carcinoma. *J Cancer Res Clin Oncol*, 2004; 130, 187-96.
 29. Sun J, Hemler ME. Regulation of MMP-1 and MMP-2 production through CD147/extracellular matrix metalloproteinase inducer interactions. *Cancer Res*, 2001; 5, 2276-81.
 30. J Tang, HW Zhou, JL Jiang, et al. Beta1g-h3 is involved in the HAB18G/CD147-mediated metastasis process in human hepatoma cells. *Exp Biol Med (Maywood)*, 2007; 232, 344-52.
 31. Y Wang, L Yuan, XM Yang, et al. A chimeric antibody targeting CD147 inhibits hepatocellular carcinoma cell motility via FAK-PI3K-Akt-Girdin signaling pathway. *Clin Exp Metastasis*, 2015; 32, 39-53.
 32. SJ Wang, HY Cui, YM Liu, et al. CD147 promotes Src-dependent activation of Rac1 signaling through STAT3/DOCK8 during the motility of hepatocellular carcinoma cells. *Oncotarget*, 2015; 6, 243-57.
 33. HY Cui, T Guo, SJ Wang, et al. Dimerization is essential for HAB18G/CD147 promoting tumor invasion via MAPK pathway. *Biochem Biophys Res Commun*, 2012; 419, 517-22.
 34. V Miranda-Goncalves, M Honavar, C Pinheiro O, et al. Monocarboxylate transporters (MCTs) in gliomas: expression and exploitation as therapeutic targets. *Neuro Oncol*, 2013; 15, 172-88.
 35. Z Zhang, Y Zhang, Q Sun, et al. Preclinical pharmacokinetics, tolerability, and pharmacodynamics of metuzumab, a novel CD147 human-mouse chimeric and glycoengineered antibody. *Mol Cancer Ther*, 2015; 14, 162-73.
 36. F Feng, B Wang, X Sun, et al. Metuzumab enhanced chemosensitivity and apoptosis in non-small cell lung carcinoma. *Cancer Biol Ther*, 2017; 18, 51-62.
 37. H Davies, GR Bignell, C Cox, et al. Mutations of the BRAF gene in human cancer. *Nature*, 2002; 417, 949-54.
 38. MS Kinch, D Hoyer, E Patridge, et al. Target selection for FDA-approved medicines. *Drug Discov Today*, 2015; 20, 784-9.
 39. JC Hertzman, BS Eghazi. BRAF inhibitors in cancer therapy. *Pharmacol Ther*, 2014; 142, 176-82.
 40. I Okamoto. Epidermal growth factor receptor in relation to tumor development: EGFR-targeted anticancer therapy. *FEBS J*, 2010; 277, 309-15.
 41. RJ Roskoski. A historical overview of protein kinases and their targeted small molecule inhibitors. *Pharmacol Res*, 2015; 100, 1-23.
 42. M MacFarlane, AC Williams. Apoptosis and disease: a life or death decision. *EMBO Rep*, 2004; 5, 674-8.
 43. A Talaiezhadeh, F Jalali, H Galehdari, et al. Time depended Bcl-2 inhibition might be useful for a targeted drug therapy. *Cancer Cell Int*, 2015; 15, 105.
 44. CK Kontos, MI Christodoulou, A Scorilas. Apoptosis-related BCL2-family members: Key players in chemotherapy. *Anticancer Agents Med Chem*, 2014; 14, 353-74.
 45. A Kamal, S Faazil, MS Malik. Apoptosis-inducing agents: a patent review (2010- 2013). *Expert Opin Ther Pat*, 2014; 24, 339-54.
 46. Pieper AA, Verma A, Zhang J, et al. Poly (ADP-ribose) polymerase, nitric oxide and cell death. *Trends Pharmacol. Sci*, 1999; 4, 171-81.
 47. Li kou, Young cheun, Myong Chul Koag. Synthesis of 14', 15'-dehydro-ritterazine Y via reductive and oxidative functionalizations of hecogenin acetate. *Steroids*, 2013; 78, 304-11.
 48. Li Kou, Seongmin Lee. Unexpected opening of steroidal E-ring during hypiodite-mediated oxidation. *Tetrahedron Letters*, 2013; 54, 4106-9.